

Modeling the ortho-to-para abundance ratio of cyclic C₃H₂ in cold dense cores

I. H. Park¹, V. Wakelam², and E. Herbst³

¹ Chemical Physics Program, The Ohio State University, Columbus, OH 43210 USA
e-mail: ihpark@mps.ohio-state.edu

² Department of Physics, The Ohio State University, Columbus, OH 43210 USA
e-mail: wakelam@mps.ohio-state.edu

³ Departments of Physics, Chemistry and Astronomy, The Ohio State University, Columbus, OH 43210 USA
e-mail: herbst@mps.ohio-state.edu

Received 2005; accepted 2005

ABSTRACT

Aims. We report a detailed attempt to model the ortho-to-para abundance ratio of *c*-C₃H₂ so as to reproduce observed values in the cores of the well-known source TMC-1. According to observations, the ortho-to-para ratios vary, within large uncertainties, from a low of near unity to a high of approximately three depending on the core.

Methods. We used the osu.2003 network of gas-phase chemical reactions augmented by reactions that specifically consider the formation, depletion, and interconversion of the *ortho* and *para* forms of the *c*-C₃H₂ and its precursor ion *c*-C₃H₂⁺. We investigated the sensitivity of the calculated ortho-to-para ratio for *c*-C₃H₂ to a large number of factors.

Results. For the less evolved cores C, CP, and D, we had no difficulty reproducing the observed ortho-to-para ratios of 1-2. In order to reproduce observed ortho-to-para ratios of near three, observed for the evolved cores A and B, it was necessary to include rapid ion-catalyzed interconversion processes.

Key words. Astrochemistry – ISM: molecular abundances – ISM: clouds – ISM: molecules – ISM: Individual objects: TMC1

1. Introduction

Cyclopropenylidene, *c*-C₃H₂, is a widely-distributed abundant organic ring molecule in the interstellar medium (Thaddeus et al. 1985; Matthews & Irvine 1985; Vrtilek et al. 1987). Its “linear” isomer, propadienylidene (*l*-C₃H₂), has also been observed in a number of sources, albeit at lower abundance (Cernicharo et al. 1999; Fossé et al. 2001; Teyssier et al. 2005; Cernicharo et al. 1991; Kawagushi et al. 1991; Turner et al. 2000). For each isomer, two equivalent H nuclei, of spin 1/2, couple to generate *ortho* (nuclear spin = 1) and *para* (nuclear spin = 0) species with spin statistical weights of 3 and 1, respectively. The nuclear spin wave functions of the *ortho* states are symmetric to exchange of the protons whereas those of the *para* states are anti-symmetric. Since the Pauli exclusion principle requires total wave functions to be antisymmetric to exchange of protons, the symmetry of the rotational wave function of the molecule to exchange must be antisymmetric for *ortho* spin states and symmetric for *para* spin states if the ground electronic state is symmetric to ex-

change. The dependence of the exchange symmetry of the rotational state on the rotational quantum numbers depends on the structure of the molecule and on the symmetry of the electronic state (Townes & Schawlow 1975). Moreover, the conversion of molecular species from rotational levels with *ortho* spin functions to those with *para* spin functions does not occur efficiently if at all by radiative or non-reactive collisional mechanisms in the gas, so that, in the absence of reaction (or strong binding with a surface), the sets of rotational levels with *ortho* and *para* spin functions can be regarded as distinct species.

The cyclic isomer of C₃H₂ has been observed in the interstellar medium in transitions belonging to both spin states: for *o*-C₃H₂, the observed lines include the *b*-type transitions 1₁₀-1₀₁, 2₁₂-1₀₁, 3₁₂-3₀₃, 3₂₁-3₁₂ and 3₃₀-3₂₁ at 18.3, 85.3, 83.0, 44.1, and 27.1 GHz respectively, whereas for *p*-C₃H₂, the observed *b*-type transitions include 2₀₂-1₁₁, 2₁₁-2₀₂, 2₂₀-2₁₁ and 3₂₂-3₁₃ lines at 82.1, 46.8, 21.6, and 84.7 GHz respectively (Cernicharo et al. 1999; Matthews & Irvine 1985; Thaddeus et al. 1985; Takakuwa et al. 2001; Madden et al. 1989; Morisawa et al. 2005). With this many transitions, ortho-to-para ratios of reasonably high accuracy can be obtained, al-

lowing a detailed understanding of the chemical processes involved and possibly even the history of the source.

In the terrestrial laboratory one often refers to two-types of mixtures for *ortho* and *para* species involving two protons: the common *normal* variety, in which the ortho-to-para ratio is three, and the *equilibrium* variety, in which the ortho-to-para ratio reflects thermal equilibrium. In the interstellar medium, however, the ortho-to-para ratio at low temperatures is probably governed by kinetic rather than thermodynamical considerations, including processes on grains, and is likely to be time-dependent and may even reflect the original circumstances of the molecule formation (Tiné et al. 2003; Takahashi 2001; Le Bourlot 2000). In fact, detailed estimates of the steady-state interstellar ortho-to-para H₂ ratio at 10 K show that it is approximately 10⁻³ (Pagani et al. 1991; Le Bourlot 1991; Le Bourlot et al. 1999), far higher than the equilibrium value of 3 × 10⁻⁷.

Molecular hydrogen is unique in showing such a strong deviation between thermal and normal values for the *o/p* ratio at temperatures in the vicinity of 10 K. For heavier species, this deviation is much smaller because more levels of each spin modification are thermally populated so that values of ≈ 3.0 for the thermal ratio pertain to quite low temperatures. For H₂CO, (Dickens & Irvine 1999; Kahane et al. 1984), this ratio is reached at temperatures as low as ≈ 15 K, while for *c*-C₃H₂, the ratio is reached under thermal conditions at temperatures under 5 K (Takakuwa et al. 2001). Nevertheless, the actual *o/p* ratio in cold dense interstellar sources is determined by kinetic considerations and may well be significantly under three at 10 K clouds for heavy species with two equivalent protons, as detected for the species H₂CO, H₂CS, and H₂CCO (Dickens & Irvine 1999; Minh et al. 1991; Ohishi et al. 1991).

Although the ortho-to-para abundance ratio of *c*-C₃H₂ had been studied observationally in TMC-1 by Madden et al. (1989) and Takakuwa et al. (2001) and in L1527 by Takakuwa et al. (2001), this work is motivated by the recent observational work of Morisawa et al. (2005) (hereafter, MFK), who measured the ratio in a more comprehensive manner for the six different cores within the TMC-1 ridge: A, B, C, D, CP, and E. Their measured ratios range from 1.4±0.7 (TMC-1D and CP) to 3.0±1.5 (TMC-1A and B). Note that Core D sometimes refers to some substructure near the CP condensation, in which case, it can be referred to as CP-b (Hirahara et al. 1992), but other authors have used Core D to be the same as Core CP (Hartquist et al. 2001), which is the very well-studied core where the abundances of complex carbon chains peak (Smith et al. 2004). In addition, TMC1-B is the so-called ammonia peak (Howe et al. 1996). The current understanding is that some of the cores (e.g. Core B) are more evolved than others (e.g. Core CP) although the cause of the differential evolution is not fully understood (Hartquist et al. 1996; Howe et al. 1996; Markwick et al. 2000).

Table 1 shows the observed *o/p* abundance ratios of cyclic *c*-C₃H₂ in the six cores (MFK) along with measured fractional abundances (X) of *o*-C₃H₂ with respect to H₂ and estimated ages of the cores. Although the determination of cloud ages is still contentious, there is a sufficient consensus concerning the chemical indicators of age to use the results in this paper. It can

be seen that, as noted by MFK, the ortho-to-para ratio seems to be generally correlated with the evolution of the core; i.e., for all cores other than Core E, the older the core chemically, the higher the ortho-to-para ratio within large uncertainties, especially for the higher ortho-to-para ratios.

MFK used a simple model of a small number of gas-phase chemical reactions to understand their measured abundance ratios in terms of the evolution of the cores. They showed that the ortho-para chemistry of *c*-C₃H₂ is rather simple compared with other heavy molecules that have been studied, so that a complete understanding of the *o/p* abundance ratio is possibly obtainable. Our detailed model is based on their simple one, with, as discussed below, the important reactions for the formation and depletion of the *ortho* and *para* forms of *c*-C₃H₂ and its protonated ion precursor embedded in a large chemical network.

In this paper, we report the results of our detailed gas-phase chemical model of the ortho-to-para abundance ratio of *c*-C₃H₂. The remainder of this paper is divided as follows. In Section 2 we discuss the details of our gas-phase chemical model, while in Section 3, we illustrate our results for the ortho-to-para ratio of *c*-C₃H₂ as a function of time. We also compare our results with the model of MFK. As will be seen, our standard results are not capable of producing *o/p* ratios greater than 2.1, so we consider some additional direct chemical processes that can convert the *para* form of the ring molecule to its *ortho* form. With these processes, we are able to account for the possibly high *o/p* ratio in the more evolved cores. We then subject our results to an uncertainty analysis. Section 4, the discussion, concludes the paper.

2. The model

The chemical reaction network used for this work is an updated version of the .2003 gas-phase network (Smith et al. 2004). Several versions of this network are now available at the URL <http://www.physics.ohio-state.edu/~eric/research.html>. For this work, we added several other modifications. First, and most importantly, we added reactions to account for the chemistry of both forms of *c*-C₃H₂ and its protonated precursor *c*-C₃H₃⁺ (see below). Note that this ion has three-fold symmetry so that its protons are all indistinguishable: the *ortho* form has a total nuclear spin of 3/2, while the two *para* forms (Oka 2004) each have a total nuclear spin of 1/2, although only one of these exists for a given rotational state (Townes & Schawlow 1975). Secondly, we added new experimental information on the neutral products and total rate coefficients for dissociative recombination reactions involving several hydrocarbon ions (Larson et al. 1998; Semaniak et al. 1998; Kalhori et al. 2002; Derkatch et al. 1999; Mitchell et al. 2003). Thirdly, we ignored the existence of the linear isomer of lower abundance - *l*-C₃H₂ - to simplify the problem for *c*-C₃H₂.

2.1. Formation and destruction of *c*-C₃H₂

The formation of *c*-C₃H₂ begins with the radiative association of C₃H⁺ with H₂ to produce the precursor ion *c*-C₃H₃⁺.

Table 1. Some c-C₃H₂ observations of the cores in the TMC-1 ridge

Source	Observed <i>o/p</i> Ratio ^b	Observed X(<i>o</i> -C ₃ H ₂) × 10 ⁻¹⁰ ^b	Estimated Age (yr)
<i>Cores with high o/p ratio</i> ...			
TMC-1A	3.0 ^{+2.2} _{-1.3}	7.5 ⁺¹² _{-5.4}	~ 10 ⁶ ^b
TMC-1B	3.0 ^{+1.7} _{-1.1} ; 3.0 ± 0.16 ^c	7.9 ⁺¹² _{-5.4}	~ 10 ⁶ -10 ⁷ ^h
TMC-1E	2.8 ^{+2.1} _{-1.2}	4.6 ^{+7.7} _{-3.4}	~ 10 ⁴ -10 ⁵ ^{a,b}
<i>Cores with low o/p ratio</i> ...			
TMC-1C	1.8 ^{+0.9} _{-0.6} ; 2.4 ± 0.1 ^c	6.0 ^{+8.4} _{-4.0} ; 13 ^e	~ 10 ⁵ ^b
TMC-1CP	1.4 ^{+0.9} _{-0.5} ; 2.56 ± 0.31 ^d	16 ⁺³² ₋₁₃ ; 57 ^d	~ 10 ⁵ ^{f,g} ; 6 × 10 ⁴ ^h
TMC-1D ^a	1.4 ^{+1.1} _{-0.7}	8.3 ⁺¹⁹ _{-6.9}	6 × 10 ⁴ ^h

^a Hirahara et al. (1992). Core D is Core CP-b according to this source.

^b MFK unless noted. The fractional abundances X of *o*-C₃H₂ are with respect to H₂. Based on the MFK logarithmic observables, we carried out slightly different error calculations, because here $\Delta \log X$ is not much less than 1, so that two 1 σ random errors $\Delta X_- \approx \Delta X_+$ should be calculated (Wakelam et al. 2005).

^c Takakuwa et al. (2001)

^d Madden (1990)

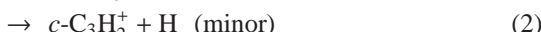
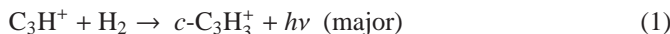
^e Cox et al. (1989)

^f Saito et al. (2002)

^g Smith et al. (2004)

^h Hartquist et al. (2001)

This association is not the only reaction these two reactants undergo; the H-atom transfer channel to form *c*-C₃H₂⁺ + H may be competitive, although it is unclear whether or not the reaction is endothermic (Herbst et al. 1984; Maluendes et al. 1993). In the .2003 (Smith et al. 2004) and .99 networks (Le Teuff et al. 2000) the H-atom transfer is assumed to be a minor channel at 10 K. Once the cyclic C₃H₃⁺ ion is formed, its major destruction is by dissociative recombination, one channel of which leads to *c*-C₃H₂:



where the \dots in reaction (4) refer to the fact that the additional products H + H or H₂ have not been explicitly determined by experiment. According to the recent experiment performed by Angelova et al. (2004) on the dissociative recombination of C₃H₃⁺, product channels containing molecules with three carbon atoms account for 90.7% of the products. The experiment was not able to differentiate among the C₃H_{*m*} species, nor to determine if linear or cyclic species were present, so the branching ratio for the important products *c*-C₃H₂ + H remains a free parameter.

Once produced, *c*-C₃H₂ is destroyed by reactions with a variety of ions while its precursor ion can be destroyed by neutral

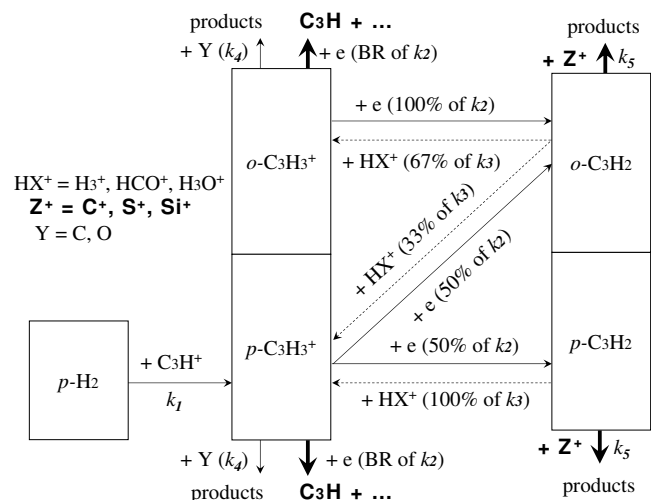
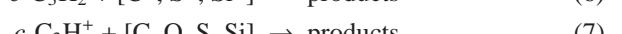
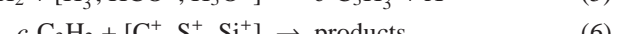
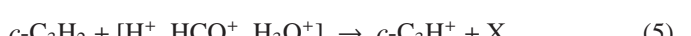


Fig. 1. Dominant reaction diagram for the standard models. Some processes not considered by MFK are indicated by bold-face.

species in addition to dissociative recombination:



Note that from now on, the cyclic designation *c*- will be understood and not written explicitly.

One can see that in the absence of C₃H₂ reactions involving ions other than protonating ones, of ion-atom reactions involving C₃H₃⁺, and of dissociative recombination of this ion to form

any products other than C₃H₂, there is a quasi-cycle or loop in which once the protonated ion C₃H₃⁺ is formed, dissociative recombination and protonation serve only to convert these species into one another. As these processes occur, ortho-para conversion also occurs, as we shall now discuss.

2.2. Para-to-ortho conversion: standard and alternative models

The dominant set of reactions involving the ortho/para chemistry of C₃H₂ in our *standard models*, based on the model of MFK, is listed in Table 2 along with additional reactions for two *alternative models*. The important reactions in the standard approach are shown in Fig. 1 where the rate coefficients and their numerical subscripts are defined in the table. In Table 2, the reactions are on the far left, with the rate coefficients and branching fractions next to them. The branching fractions are written in terms of the rate coefficients, which are numbered according to their position in the table. Reactions in the simple model of MFK are indicated by a dark circle.

The basic structure of the reaction scheme commences with the production of *p*-C₃H₃⁺ by radiative association because the H₂ reactant, as discussed in the Introduction, is overwhelmingly *para* in nature for cold clouds. Thus the zero nuclear spin of H₂ and the spin of the individual proton in C₃H⁺ can combine only to form a resultant nuclear spin of 1/2, which corresponds to a *para* form of C₃H₃⁺. Once *p*-C₃H₃⁺ is formed, it undergoes dissociative recombination to form both *p*- and *o*-forms of C₃H₂ (as well as other neutral products). The C₃H₂ species can then undergo protonation reactions with a variety of ions designated HX⁺; these processes lead to both *ortho* and *para* versions of the protonated ion. As the loop reactions continue, sizable proportions of *o*-C₃H₂ are built up. In competition with the production of *ortho* species within the loop, other reactions serve to force the system to exit the loop, including (i) non-protonating ion-molecule reactions with C₃H₂, (ii) dissociative recombination of C₃H₃⁺ to form products other than C₃H₂, (iii) ion-atom reactions involving C₃H₃⁺. Of course, in a complex model, some of the products formed outside of the loop can eventually lead to reactions such that the products are once again C₃H₂ and its protonated ion. In addition to the cycle of protonation and dissociative recombination, there may also be direct conversion processes; such processes will be discussed later but can be seen in Table 2 as part of our alternative models.

In order to determine the selection rules and branching ratios for ortho/para products in protonation and dissociative recombination, we have used the approach of Oka (2004), in which angular momentum algebra is applied to the addition of the nuclear spins of the reactants to determine the spin angular momenta of the intermediate complex, which then dissociates into product states of given spin angular momentum. In the language of the rotation group, if one considers the two reactants to have proton nuclear spins of I_1 and I_2 , the combined spin state can be written as $\mathcal{D}_{I_1} \otimes \mathcal{D}_{I_2}$. This state leads to the intermediate state $\mathcal{D}_{I_1+I_2} \oplus \mathcal{D}_{I_1+I_2-1} \oplus \dots \oplus \mathcal{D}_{|I_1-I_2|}$, which means that the complex can have total proton spin angular moment

ranging from $I_1 + I_2$ down to $|I_1 - I_2|$. Each of these angular momenta can then dissociate into product spin states given by angular momentum rules (Oka 2004). The approach of Oka is most valid for processes in which many rotational states of the products can be produced. These processes can be exothermic reactions or even thermoneutral reactions if the energy is sufficiently high. In this limit, one need not worry much about the rotational quantum number J , since many different J states are produced. For low-temperature thermoneutral processes, on the other hand, where a small number of J states may be produced, the role of the individual J states needs to be taken into account in a comprehensive quasi-phase-space theoretical approach (Herbst 1982; Gerlich 1990; Gerlich & Schlemmer 2002). Although the approach of Oka (2004) lends itself naturally to the idea of a reaction intermediate in which all protons are indistinguishable from one another and can be facilely exchanged during the life of the complex, it is also possible to remove this assumption. In fact, in our use of the treatment for the ion H₃⁺, we assume that the protonation reactions occur by simple transfer of a proton rather than formation of a complex consisting of C₃H₂ and H₃⁺. Our branching fractions are the same as those used by MFK, who derived theirs with the approach of Quack (1977), which is equivalent to that of Oka (2004).

In our standard models, we do not consider direct (ion-catalyzed) interconversion processes between the *ortho* and *para* forms of C₃H₂ because competitive reactions with abundant ions that might catalyze such a conversion also occur. For example, the reaction of C₃H₂ with protons is likely to produce exothermic products such as C₃H⁺ + H₂ rather than undergo the exchange of protons needed to cause ortho/para change while the reactions with protonating ions such as HCO⁺ and H₃⁺ are likely to undergo protonation. Nevertheless, we find, as will be shown Section 3.2, that in the absence of such interconversion/exchange reactions, the calculated ortho-to-para ratio for C₃H₂ cannot be large enough to explain observed values near 3.0. So, in our alternative models we also consider interconversion of *o*- and *p*-C₃H₂ by ion-catalyzed exchange processes with the four ions H⁺, H₃⁺, H₃O⁺ and HCO⁺, the latter three occasionally being designated by HX⁺. For these processes, the approach of Oka (2004) leads to the detailed balance expression in the limit that kT exceeds the ortho-para energy difference:

$$\frac{k(p \rightarrow o)}{k(o \rightarrow p)} = \frac{k_{-i}}{k_i} = 3, \quad (8)$$

where i is an index of the four pairs of interconversion processes considered. We simplify the forward and backward processes such that the reactants produce a complex with a given rate coefficient $k = k_i + k_{-i}$; the complex then dissociates into *o*-C₃H₂ on 3/4 of the collisions and *p*-C₃H₂ on 1/4 of the collisions regardless of the initial reactants. In the theory of Oka (2004), the relevant formulae are $k(o \rightarrow p) = 1/6 k$ and $k(p \rightarrow o) = 1/2 k$ for isomerization reactions involving a proton. For the unknown rate coefficients $k_i + k_{-i}$, we choose a standard value equal to the ion-dipole collision rate. To the best of our knowledge, there is no evidence for or against the supposition that these particular ortho/para exchange reactions are not competitive with reaction. Perhaps the strongest evidence that

Table 3. Default initial conditions

Low-metal abundance	Other parameters
He	6.00(-2)
N	2.14(-5)
O	1.76(-4)
H ₂	5.00(-1)
C ⁺	7.30(-5) Temperature = 10 K
S ⁺	8.00(-8) $n_H = 2 \times 10^4 \text{ cm}^{-3}$
Si ⁺	8.00(-9) $\zeta = 1.3 \times 10^{-17} \text{ s}^{-1}$
Fe ⁺	3.00(-9) C/O ratio = 0.41
Na ⁺	2.00(-9) $A_v = 10 \text{ mag}$
Mg ⁺	7.00(-9) $\text{C}_3\text{H}_3^+ + \text{e} \xrightarrow{0.5 k_2} \text{C}_3\text{H}_2 + \text{H}$
P ⁺	3.00(-9) $\xrightarrow{0.5 k_2} \text{C}_3\text{H} + \dots$
Cl ⁺	4.00(-9)
e	7.3107(-5)

Note : a(-b) = a $\times 10^{-b}$, with respect to H abundance

Table 4. Summary of variations of standard model parameters

Parameters Varied	Range
1) C/O ratio	0.21 - 1.20
2) Metal depletion	low-metal – additional depletion of real metals by factors of 2 low-metal – high-metal
3) Cosmic-ray ionization rate ζ	$1.3 \times 10^{-18} \text{ s}^{-1} - 1.3 \times 10^{-16} \text{ s}^{-1}$
4) Gas-density n_H	$2 \times 10^3 \text{ cm}^{-3} - 2 \times 10^5 \text{ cm}^{-3}$
5) C ₃ H ₂ + H fraction	0.50 - 1.00

such processes occur is discussed in Cordinier et al. (2000), where the exchange mechanism via the complex H₅⁺ is measured to occur in the reaction between H₂ and H₃⁺ in competition with a simple proton hop.

2.3. Parameters and models: default & sets of models 1-6

In our calculations of the *o/p* abundance ratio of C₃H₂, we start with a default set of initial conditions, listed in Table 3, used with our standard model of reactions. The default model contains so-called low-metal abundances (depleted heavy elements with C/O = 0.41) with the additional assumption that the initial abundances are atomic except for hydrogen, which is molecular. In addition, the total hydrogen density is set at $n_H = 2 \times 10^4 \text{ cm}^{-3}$, the temperature at 10 K, the visual extinction at 10 mag, and the cosmic-ray ionization rate ζ at $1.3 \times 10^{-17} \text{ s}^{-1}$. Finally the unknown branching fraction for the dissociative recombination of C₃H₃⁺ is set so that the products C₃H₂ + H and C₃H + ... are produced in equal amounts. The chemistry is followed with a single-point model under constant physical conditions.

In an attempt to determine how the computed *o/p* abundance ratio for C₃H₂ vs time depends upon an assortment of

parameters, we have varied the C/O elemental ratio, the degree of metallicity, the cosmic ray ionization rate, and the gas density, as well as the neutral product branching ratio of the dissociative recombination reaction of the ion C₃H₃⁺. These parameters affect how long the C₃H₂ ortho-para system can stay in the loop shown in Fig. 1. Table 4 shows the range of the parameters considered in this work for our standard list of additional reactions. For each parameter, a number of different runs was attempted within the ranges listed in the table. The variation of parameters with our alternative model is more restrictive, as will be discussed in Section 3.2.

3. Results

3.1. Default and other standard sets of models vs observation

The calculated *o/p* ratio for C₃H₂ as a function of time in our default model is shown in panel a) of Fig. 2. Superimposed are the observational results for the cores in TMC-1; e.g., Cores CP(D) and C, for which very short lifetimes are believed to pertain, Core A, with an intermediate lifetime, and Core B, for which a long lifetime of $\approx 10^7 \text{ yr}$ is normally suggested. Core E is included although its lifetime is rather uncertain: the high *o/p* ratio suggests some evolution, but the measured NH₃/CCS ratio is low (Hirahara et al. 1992), suggesting a young chemical age (MFK). Uncertainties in the lifetimes are large and not included in the figure.

With our default model, we obtain the result that the *o/p* ratio is near unity at times relevant to Cores CP(D) and C, in reasonable if not excellent agreement with observed ratios, but never increases very much with time, reaching a steady-state value under 1.5, in some disagreement with the measured ratios of $3.0^{+2.2}_{-1.3}$ and $3.0^{+1.7}_{-1.1}$ for Cores A and B, where we have used our recalculated uncertainties (see footnote in Table 1). The calculated fractional abundance for *o*-C₃H₂ is shown in panel c) of Fig. 2, where it can be seen that the agreement with the lower age cores is fair, with the model result being somewhat high, is excellent for Core A, but is particularly poor for Core B. The calculated result is a typical one for pseudo-time-dependent models, in which most organic species have high abundance only at so-called “early time.” If the age of Core B were 10^6 yr , then the disagreement would be eliminated for the fractional abundance of *o*-C₃H₂ although the disagreement with the observed *o/p* ratio would remain. Using the abundance ratio of NH₃ to CCS as the criterion of chemical age, MFK considered the age of core B to be comparable to Core A, but this analysis is unclear because the abundance ratio is indeed larger for Core B, although not by a huge factor.

Given the probable disparity between the results of the default model and observations for the *o/p* ratio at long times, we varied the five parameters discussed in Section 2.3 over the ranges listed in Table 4 to obtain a variety of results with the standard sets of models 1-6. Note that the highest density used is similar to the densities derived by MFK; our default value is the more traditional one. The result was little change in the quantities of interest except when we varied the branching ratio for the products of the dissociative recombination branching

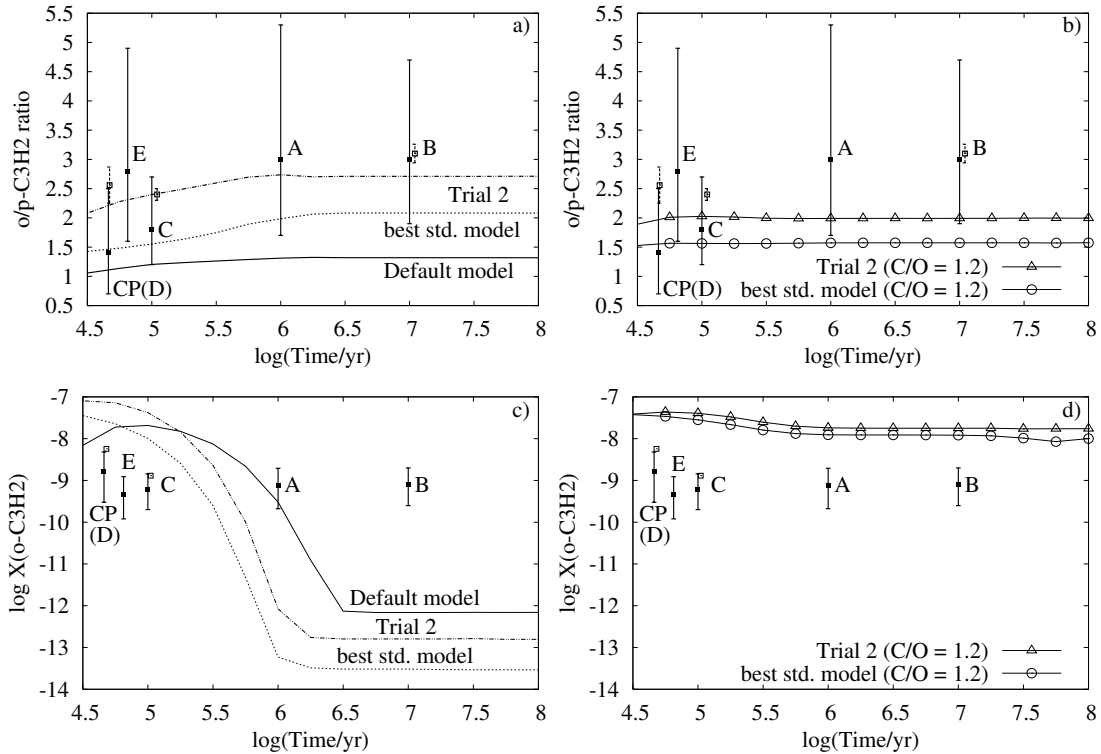


Fig. 2. Calculated values of the ortho-to-para C₃H₂ abundance ratio (panels a and b) and fractional abundance of *o*-C₃H₂ (panels c and d) with respect to H₂ vs time compared with observed values in the cores of TMC-1. Note that the superimposed solid (MFK) and dotted (Madden 1990; Cox et al. 1989) error bars are from different observations. See text for explanation of models used.

fraction. When the branching fraction for the products C₃H₂ + H is increased to unity, the calculated *o/p* ratio for C₃H₂ increases to about 1.9 at steady state. An increase in the ratio to about 2.1 can be obtained with the following other parameters: C/O elemental ratio = 0.2, metal depletion a factor of two, no change in the value of ζ , and a higher density of 2×10^5 cm⁻³. The results of this model, labeled our “best” standard model, for the *o/p* ratio and abundance of *o*-C₃H₂ are shown in panels a) and c) of Fig. 2. The results for the *o/p* ratio are now barely within the large observational error bars, although the results for *o*-C₃H₂ are still poor for the evolved core B, and would be poor even if the age of this core were reduced by an order of magnitude. As is well-known, the only way to increase the calculated abundance of carbon-chain type species at late times is to use a carbon-rich elemental abundance. With our best standard model changed only so that the elemental carbon-to-oxygen ratio C/O = 1.2, we get the results shown in panels b) and d) of Fig. 2, where it can be seen that the observed fractional abundance of *o*-C₃H₂ as a function of core age is reasonably reproduced albeit somewhat high at all times with respect to the most recent measurements (MFK), although the *o/p* ratio has lost all of its time dependence. Nevertheless, the model results for the *o/p* ratio lie (barely) within the observational errors except for Core B.

3.2. Models with direct interconversion

In order to reach an *o/p* ratio of ≈ 3.0 at steady-state, we included direct interconversion between the *para* and *ortho* forms of C₃H₂, as shown in Table 2. For the alternative approach known as “Trial 2”, the conversion reactions are actually assumed to be more rapid than protonation by a factor of five for the protonating ions HX⁺. The results of Trial 2 using the same set of parameters as used for the best standard model are also shown in panels a) and c) of Fig. 2. Here the calculated ratio reaches a steady-state value of near 2.7 and is in good agreement with observation over the complete time range. On the other hand, the agreement with the fractional abundance of *o*-C₃H₂ for late times (Core B) is once again poor, even if the age of this core is reduced to 10⁶ yr. If, to remedy this latter deficiency, the C/O elemental ratio is set to 1.2, then the fractional abundance of *o*-C₃H₂ at late times is in fair agreement with the observed value in Core B but the calculated *o/p* ratio never rises above 2.1. If the less dramatic assumption is made that the rate coefficients for interconversion are the same as for protonation (“Trial 1”), then the steady-state *o/p* ratio reaches a value of 2.5, also in reasonable agreement with observation in the older cores. But the same problems occur with the fractional abundance of *o*-C₃H₂ as occur for Trial 2. Models with a C/O elemental ratio of 1.0 are no more successful. We conclude that no simple pseudo-time-dependent model of the type considered here explains all of the data.

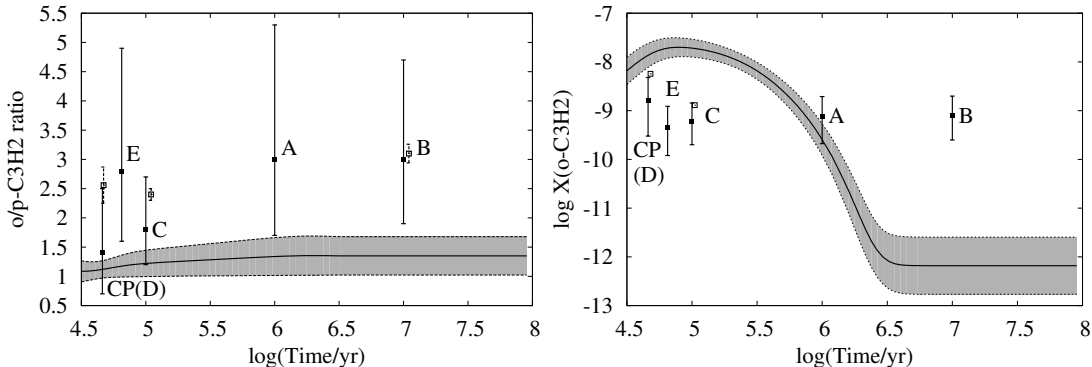


Fig. 3. Calculated uncertainties in the ortho-to-para C₃H₂ abundance ratio (left panel) and fractional abundance of *o*-C₃H₂ (right panel) for the default model case.

3.3. Comparison with simple model

MFK developed a simple model to calculate the *o/p* C₃H₂ abundance ratio. In their model only a few types of reactions are considered (see • marks in Table 2). In the limit of steady state, the ratio can be shown to be

$$\frac{n(o\text{-C}_3\text{H}_2)}{n(p\text{-C}_3\text{H}_2)} = \frac{(5 + 3\phi) \times \frac{n(o\text{-H}_2)}{n(p\text{-H}_2)} + 3\phi + 3}{(1 + \phi) \frac{n(o\text{-H}_2)}{n(p\text{-H}_2)} + \phi + 3} \xrightarrow{o/p\text{-H}_2 \sim 0} \frac{3(\phi + 1)}{\phi + 3} \quad (9)$$

where ϕ is $k_{DR}n(e)/k_{ion\text{-}Y}n(Y)$, the ratio of the product of the dissociative recombination rate coefficient of C₃H₃⁺, k_{DR} , and the electron abundance, $n(e)$, divided by the product of the rate coefficient for ion-atom reactions of C₃H₃⁺, $k_{ion\text{-}Y}$, and the abundance of reactive atoms, $n(Y)$. The parameter ϕ is essentially related to the ability of the reactants to stay in the loop shown in Fig. 1. If one makes the assumption that H₂ is overwhelmingly *para* in nature, then the *o/p* ratio of C₃H₂ is determined solely by the parameter ϕ , with a large value of ϕ leading to an *o/p* ratio of 3 and a small value of ϕ leading to a ratio of 1. With the values for $n(Y)$ and $n(e)$ assumed by MFK, the former ratio pertains at steady state; their assumptions contain a rather high fractional abundance for electrons, which we would associate only with the high-metal case of elemental abundances. With the more standard low-metal case, the computed ratio becomes very close to unity, in agreement with our more detailed results. With the high-metal-type parameters chosen by MFK, their time-dependent calculation shows that the *o/p* ratio of C₃H₂ shifts dramatically from 1 to 3 at some intermediate time.

But there are two omissions in the theory leading to the simple steady-state formula for the *o/p* ratio: (i) destructive reactions involving C₃H₂ with a host of non-protonating ions such as C⁺ that make the system leave the loop, and (ii) dissociative recombination leading to products other than C₃H₂ + H, which again have the effect of forcing the system to leave the loop. The effect of including both of these processes in the high-metal case makes the simple steady-state for the *o/p* ratio a more complex one and reduces the calculated ratio to values close to those calculated in our more detailed approach. In other words, it is still difficult to produce large *o/p* abundance ratios in the absence of direct inter-conversion reactions.

3.4. The role of uncertainties in rate coefficients

Another important aspect that we considered in our study is the uncertainty in the rate coefficients. Using the method described in Wakelam et al. (2005), we computed errors both in the fractional abundance of *o*-C₃H₂ and in the *o/p*-C₃H₂ abundance ratio for the default model. Briefly, this method consists of randomly generating new sets of reactions of the 2003 database within their uncertainty range using a Monte-Carlo procedure. We ran 2000 different runs which gave 2000 values of the *o*-C₃H₂ abundance and of the *o/p*-C₃H₂ ratio. The error in the abundance and ratio is defined at each time as the envelope containing 66% of the computed values (1 σ). We chose a 1 σ error because the observations are also given an observational error of 1 σ . We utilized an uncertainty of a factor of two for the rate coefficients of the reactions listed in Table 2. For the reactions of this table that have more than one product channel, we kept the branching ratio constant, because they were derived from theory and, as a consequence, have no statistical error.

We found a maximum error of ± 0.4 for the *o/p*-C₃H₂ ratio at 10⁴ yr. This error decreases to ± 0.2 at 10⁵ yr before increasing again to ± 0.3 after 10⁶ yr. As shown in Fig. 3, the computed uncertainty in the ratio is not large enough to significantly affect any of our conclusions. The computed error in the fractional abundance of *o*-C₃H₂ increases with time. Specifically, the error domain is [X_{*o*-C₃H₂/1.5, 1.5X_{*o*-C₃H₂]_{at 10⁴ yr and [X_{*o*-C₃H₂/4, 4X_{*o*-C₃H₂]_{at 10⁷ yr. In this case again (see Fig. 3), the computed uncertainty does not improve the agreement with observation significantly.}}}}}}

4. Discussion and Conclusion

New observations by MFK of the ortho-to-para abundance ratio for the cyclic isomer of C₃H₂ in the six cores of TMC-1 indicate that this ratio is under 2.0 for two of three cores thought to be chemically young and is closer to the thermal value of 3.0 for those cores thought to be chemically more evolved. The parameter used to determine chemical age is the abundance ratio of NH₃ to that of CCS. The *o/p* ratio is determined by a chemistry in which the cyclic ion C₃H₃⁺ is formed initially solely in its *para* state, but by a process of dissociative recombination and re-protonation, a significant ortho/para abundance

ratio, near the thermal value of 3.0, can be built up given sufficient time for high-metal abundances if competitive reactions are not dominant. Although a simple model by MFK indicates agreement with their observations for five out of six cores if high-metal abundances are used, our more detailed calculations with an extended version of the 2003 network of reactions do not give such a definitive result, mainly because of competitive processes. In fact, with standard parameters varied over rather wide ranges, we find it difficult to obtain *o/p* ratios exceeding 2.0 at any time.

We are able to calculate higher *o/p* ratios for C₃H₂ only if we assume that the *ortho* and *para* forms of this species can be converted into one another by exchange processes involving H⁺ and protonating ions HX⁺. This assumption is based on some experiments involving H₃⁺ by Cordinnier et al. (2000) but here runs up against the problem that both H⁺ and HX⁺ will likely react with C₃H₂ and the competition between reaction and *ortho/para* conversion may well favor the former. Thus, there is still no definitive chemical proof that gas-phase processes can produce *ortho/para* ratios for cyclic C₃H₂ near the thermal value of 3.0. If, then, the observational values in this range are sufficiently accurate to distinguish correctly between low and high ratios, either the exchange reactions we consider between *o*-C₃H₂ and *p*-C₃H₂ do occur and are actually favored over reaction, our branching fractions or other aspects of the gas-phase chemistry are in error, or one must consider gas-grain interactions. Future observations with a lower uncertainty will help to determine which if any of these choices is the correct one. Even if the *o/p* ratio is reproducible by pseudo-time-dependent models of the type considered here, we must realize that the fractional abundance of the cyclic species tells a different story.

Acknowledgements. We thank Prof. Momose's group (University of British Columbia) for providing the TMC-1 observational data and their manuscript prior to submission. E.H., I.-H. P., and V.W. acknowledge the support of the National Science Foundation (US) for support of our research program in astrochemistry. We thank the Ohio Supercomputer Center for computer time on their SV1 machine.

References

Angelova, G., Novotny, O., Mitchell, J. B. A. et al. 2004, *Int. J. Mass. Spect.*, 235, 7

Cernicharo, J., Gottlieb, C. A., Guélin, M. et al. 1991, *ApJ*, 368, L39

Cernicharo, J., Cox, P., Fossé, D., & Güsten, R. 1999, *A&A*, 351, 341

Cordinnier, M., Uy, D., Dickson, R. M. et al. 2000, *J. Chem. Phys.*, 113, 3181

Cox, P., Walmsley, C. M., & Güsten, R. 1989, *A&A*, 209, 382

Derkatch, A. M., Al-Khalili, A., Vikor, L., et al. 1999, *J. Phys. B: At. Mol. Opt. Phys.*, 32, 3391

Dickens, J. E., & Irvine, W. M. 1999, *ApJ*, 518, 733

Fossé, D., Cernicharo, J., Gerin, M., & Cox, P. 2001, *ApJ*, 552, 168

Gerlich, D. 1990, *J. Chem. Phys.*, 92, 2377

Gerlich, D., & Schlemmer, S. 2002, *P&SS*, 50, 1287

Hartquist, T. W., Williams, D. A., & Caselli, P. 1996, *Ap&SS*, 238, 303

Hartquist, T. W., Williams, D. A., & Viti, S. 2001, *A&A*, 369, 605

Herbst, E. 1982, *A&A*, 111, 76

Herbst, E., Adams, N. G., & Smith, D. 1984, *ApJ*, 285, 618

Hirahara, Y., Suzuki, H., Yamamoto, S., et al. 1992, *ApJ*, 394, 539

Howe, D. A., Taylor, S. D., & Williams, D. A. 1996, *MNRAS*, 279, 143

Kahane, C., Frerking, M. A., Langer, W. D., Encrenaz, P., & Lucas, R. 1984, *A&A*, 137, 211

Kalhori, S., Viggiano, A. A., Arnold, S. T. et al. 2002, *A&A*, 391, 1159

Kawagushi, K., Kaifu, N., Hirahara, Y., et al. 1991, *PASJ*, 43, 607

Larson, Å., Le Padellec, A., Semaniak, J. et al. 1998, *ApJ*, 505, 459

Le Bourlot, J. 1991, *A&A*, 242, 235

Le Bourlot, J. 2000, *A&A*, 360, 656

Le Bourlot, J., Pineau des Forêts, G. & Flower, D. R. 1999, *MNRAS*, 305, 802

Le Teuff, Y. H., Millar, T. J., & Markwick, A. J. 2000, *A&AS*, 146, 157

Madden, S. C. 1990, PhD thesis, Univ. of Mass., Amherst, MA, USA

Madden, S. C., Irvine, W. M., Matthews, H. E., Friberg, P., & Swade, D. A. 1989, *ApJ*, 97, 1403

Maluendes, S. A., McLean, A. D., Yamashita, K., & Herbst, E. 1993, *J. Chem. Phys.*, 99, 2812

Markwick, A. J., Millar, T. J., & Charnley, S. B. 2000, *ApJ*, 535, 256

Matthews, H. E., & Irvine, W. M. 1985, *ApJ*, 298, L61 1986, *ApJS*, 307, L69

Minh, Y. C., Irvine, W. M., & Brewer, M. K. 1991, *A&A*, 244, 181

Mitchell, J. B. A., Rebrion-Rowe, C., Le Garrec, J. L., et al. 2003, *Int. J. Mass Spec.*, 227, 273

Morisawa, Y., Fushitani, M., Kato, Y., et al. 2005, *ApJ*, submitted (MFK)

Ohishi, M., Kawaguchi, K., Kaifu, N. et al. 1991, in Atoms, ions, and molecules: New results in spectral line astrophysics, ASP Conference Series (San Francisco: ASP), 16, 387

Oka, T. 2004, *J. Mol. Spect.*, 228, 635

Pagani, L., Salez, M., & Wannier, P. G. 1992, *A&A*, 258, 479

Quack, M. 1977, *Mol. Phys.*, 34, 477

Saito, S., Aikawa, Y., & Herbst, E. et al. 2002, *ApJ*, 569, 836

Semaniak, J., Larson, Å., Le Padellec, A., et al. 1998, *ApJ*, 498, 886

Smith, I. W. M., Herbst, E., & Chang, Q. 2004, *MNRAS*, 350, 323

Takahashi, J. 2001, *ApJ*, 561, 254

Takakuwa, S., Kawaguchi, K., Mikami, H., & Saito, M. 2001, *PASJ*, 53, 251

Teyssier, D., Hily-Blant, P., Gerin, M. et al. 2005, in Proc. of the dusty and molecular universe, ESA SP-577, 423

Thaddeus, P., Vrtilek, J. M., & Gottlieb, C. A. 1985, ApJ, 299, L63

Tiné, S., Williams, D. A., Clary, D. C. et al. 2003, Ap&SS, 288, 377

Townes, C. H., & Schawlow, A. L. 1975, Microwave Spectroscopy (New York: Dover)

Turner, B. E., Herbst, E., & Terzieva, R. 2000, ApJS, 126, 427

Vrtilek, J. M., Gottlieb, C. A., & Thaddeus, P. 1987, ApJ, 314, 716

Wakelam, V., Selsis, F., Herbst, E., & Caselli, P. 2005, A&A, in press

Table 2. Dominant reactions, branching ratios, and rate coefficients for the C₃H₂ ortho/para problem

Reactions	BR ^c	S				M		A		M	
		D		& S		M	1-6	T	1 ^a	T	2 ^b
		α^d	β^d	SM ^e		α	α	α	α	α	α
F											
C ₃ H ⁺ + <i>p</i> -H ₂	\rightarrow <i>p</i> -C ₃ H ₃ ⁺	k_1	3.30(-13)	1.0		•					
<i>o</i> -C ₃ H ₃ ⁺ + e	\rightarrow <i>o</i> -C ₃ H ₂ + H	$1.0 k_2$	3.15(-7)	0.5		•					
	\rightarrow <i>p</i> -C ₃ H ₂ + H	$0.0 k_2$	0	0							
	\rightarrow C ₃ H +	f	3.15(-7)	0.5							
<i>p</i> -C ₃ H ₃ ⁺ + e	\rightarrow <i>o</i> -C ₃ H ₂ + H	$0.5 k_2$	1.58(-7)	0.5		•					
	\rightarrow <i>p</i> -C ₃ H ₂ + H	$0.5 k_2$	1.58(-7)	0.5		•					
	\rightarrow C ₃ H +	f	3.15(-7)	0.5							
<i>o</i> -C ₃ H ₂ + H ₃ ⁺	\rightarrow <i>o</i> -C ₃ H ₃ ⁺ + H ₂	$0.67 k_3$	5.16(-9)	0.5		•		5.16(-9)	1/5 × 5.16(-9)		
	\rightarrow <i>p</i> -C ₃ H ₃ ⁺ + H ₂	$0.33 k_3$	2.54(-9)	0.5		•		2.54(-9)	1/5 × 2.54(-9)		
<i>o</i> -C ₃ H ₂ + H ₃ O ⁺	\rightarrow <i>o</i> -C ₃ H ₃ ⁺ + H ₂ O	$0.67 k'_3$	2.48(-9)	0.5				2.48(-9)	1/5 × 2.48(-9)		
	\rightarrow <i>p</i> -C ₃ H ₃ ⁺ + H ₂ O	$0.33 k'_3$	1.22(-9)	0.5				1.22(-9)	1/5 × 1.22(-9)		
<i>o</i> -C ₃ H ₂ + HCO ⁺	\rightarrow <i>o</i> -C ₃ H ₃ ⁺ + CO	$0.67 k''_3$	2.14(-9)	0.5				2.14(-9)	1/5 × 2.14(-9)		
	\rightarrow <i>p</i> -C ₃ H ₃ ⁺ + CO	$0.33 k''_3$	1.06(-9)	0.5				1.06(-9)	1/5 × 1.06(-9)		
D											
<i>p</i> -C ₃ H ₂ + H ₃ ⁺	\rightarrow <i>o</i> -C ₃ H ₃ ⁺ + H ₂	$0.0 k_3$	0	0		•		0	0		
	\rightarrow <i>p</i> -C ₃ H ₃ ⁺ + H ₂	$1.0 k_3$	7.70(-9)	0.5		•		7.70(-9)	1/5 × 7.70(-9)		
<i>p</i> -C ₃ H ₂ + H ₃ O ⁺	\rightarrow <i>o</i> -C ₃ H ₃ ⁺ + H ₂ O	$0.0 k'_3$	0	0				0	0		
	\rightarrow <i>p</i> -C ₃ H ₃ ⁺ + H ₂ O	$1.0 k'_3$	3.70(-9)	0.5				3.70(-9)	1/5 × 3.70(-9)		
<i>p</i> -C ₃ H ₂ + HCO ⁺	\rightarrow <i>o</i> -C ₃ H ₃ ⁺ + CO	$0.0 k''_3$	0	0				0	0		
	\rightarrow <i>p</i> -C ₃ H ₃ ⁺ + CO	$1.0 k''_3$	3.20(-9)	0.5				3.20(-9)	1/5 × 3.20(-9)		
[<i>o, p</i>]-C ₃ H ₃ ⁺ + C	\rightarrow products	k_4	1.00(-9)	0		•					
[<i>o, p</i>]-C ₃ H ₃ ⁺ + O	\rightarrow products	k'_4	4.50(-11)	0							
[<i>o, p</i>]-C ₃ H ₃ ⁺ + S	\rightarrow products	k''_4	1.00(-9)	0							
[<i>o, p</i>]-C ₃ H ₃ ⁺ + Si	\rightarrow products	k'''_4	2.00(-10)	0							
[<i>o, p</i>]-C ₃ H ₂ + C ⁺	\rightarrow products	k_5	4.20(-9)	0.5							
[<i>o, p</i>]-C ₃ H ₂ + S ⁺	\rightarrow products	k'_5	3.16(-9)	0.5							
[<i>o, p</i>]-C ₃ H ₂ + Si ⁺	\rightarrow products	k''_5	3.28(-9)	0.5							
I											
<i>o</i> -C ₃ H ₂ + H ⁺	\rightarrow <i>p</i> -C ₃ H ₂ + H ⁺	k_6		0.5				1/4 × 1.30(-8)	1/4 × 1.30(-8)		
<i>p</i> -C ₃ H ₂ + H ⁺	\rightarrow <i>o</i> -C ₃ H ₂ + H ⁺	k_{-6}		0.5				3/4 × 1.30(-8)	3/4 × 1.30(-8)		
I											
<i>o</i> -C ₃ H ₂ + H ₃ ⁺	\rightarrow <i>p</i> -C ₃ H ₂ + H ₃ ⁺	k_7		0.5				1/4 × 7.70(-9)	1/4 × 7.70(-9)		
<i>p</i> -C ₃ H ₂ + H ₃ ⁺	\rightarrow <i>o</i> -C ₃ H ₂ + H ₃ ⁺	k_{-7}		0.5				3/4 × 7.70(-9)	3/4 × 7.70(-9)		
<i>o</i> -C ₃ H ₂ + H ₃ O ⁺	\rightarrow <i>p</i> -C ₃ H ₂ + H ₃ O ⁺	k'_7		0.5				1/4 × 3.70(-9)	1/4 × 3.70(-9)		
<i>p</i> -C ₃ H ₂ + H ₃ O ⁺	\rightarrow <i>o</i> -C ₃ H ₂ + H ₃ O ⁺	k'_{-7}		0.5				3/4 × 3.70(-9)	3/4 × 3.70(-9)		
<i>o</i> -C ₃ H ₂ + HCO ⁺	\rightarrow <i>p</i> -C ₃ H ₂ + HCO ⁺	k''_7		0.5				1/4 × 3.20(-9)	1/4 × 3.20(-9)		
<i>p</i> -C ₃ H ₂ + HCO ⁺	\rightarrow <i>o</i> -C ₃ H ₂ + HCO ⁺	k''_{-7}		0.5				3/4 × 3.20(-9)	3/4 × 3.20(-9)		

Note: $a(-b) = a \times 10^{-b}$ ^a The interconversion rates are obtained as discussed in Section 2.2.^b Competitive protonation rates are suppressed by factors of 5.^c Branching ratio between ortho and para modifications obtained by angular momentum algebra (Oka 2004).^d $k = \alpha (T/300)^{-\beta} \exp(-\gamma/T)$; α is in units of cm³ s⁻¹.^e SM (Simple Model): the reactions marked with • are used in the model of MFK; with the generic forms HX⁺ and Y. See Section 3.3.^f In our standard approach, the branching fraction to form C₃H is set equal to that for C₃H₂ except for models where it is a free parameter.